FLY-BY-WIRE CONTROL OF A HELICOPTER: MULTIBODY MAIN ROTOR MODEL

S. Pastorelli, A. Battezzato, G. Mattiazzo
Department of Mechanics , Politecnico di Torino – Italy

Keywords: *Fly-by-wire, helicopters, main rotor kinematics, main rotor dynamics, multibody modeling.*

Abstract

The paper presents the multibody modeling of a helicopter fully articulated main rotor developed within a research program relevant to fly-by-wire architectures for the actuation of rotary wing aircrafts. The main aim of the model is to provide the force feedbacks on the swashplate servoactuators to evaluate their performances, both in normal and degraded conditions. Kinematics and dynamics of the device are analyzed and they are solved by means of a multibody software. In particular the paper addresses the modeling methodology and some calculation details about kinematics and aerodynamics loads. Simulation results for a reference helicopter regarding blade kinematics, rotor thrust and torque reaction, as well as swashplate servoactuators loads are presented.

1 Introduction

While fly-by-wire technology is widely applied in flight control systems of fixed wing aircrafts, it is still envisaged with great caution by the developers of helicopter rotor controls due to safety and reliability issues. Undoubtedly, loss of rotor pitch control very likely leads to a loss of the helicopter. However, the advantages of conventional mechanical signaling replacement by electrical ones carry the actuation systems designers to conceive new system architectures with extremely low safety critical failure rate.

A limited use of electrical signaling in rotor pitch control has been implemented in some helicopters, where the electrical input signals from the autopilot are converted into mechanical commands, that act on the same linkage transmitting the pilot input. These systems, however, are subordinated to the pilot commands and they can be overridden in case of failure. The transition towards fly-by-wire architectures on helicopters has firstly undertaken by Eurocopter, that employed a fly-by-wire control system on their NH90 helicopter [1]. At the same time, fly-by-wire systems have been considered by Sikorsky, that has built a demonstrator, known as H92 [2], while a fly-by-wire version of their Blackhawk is under development.

A research program on system architectures for fly-by-wire rotary wing aircrafts has been carried out by the Mechatronics and Servosystems Research Group of the Department of Mechanics, Politecnico of Turin. The program is devoted to conceive, analyze and test electrohydraulic servosystems for the fly-by-wire actuation of a helicopter main rotor.

To achieve highest safety and reliability standards, hydraulic actuators matched together in tandem or in parallel arrangements have been considered to control the position of the swashplate, inside system architectures with two independent power supplies and at least three independent electrical lanes. Developing the different alternative system architectures two requirements are taken into particular account: the systems should be fault tolerant to a jam of the hydraulic control valves and force-fighting between redundant actuators must be minimized.

The performance evaluation of a fly-by-wire actuation system, both in normal and degraded conditions, that is the transient following a failure, with detection and

consequent reconfiguration of the system, can be carried out by modeling the system, its control law and the devices that interact with it in the working environment. For a helicopter main rotor, the hydraulic actuator controls the swashplate position according to the cyclic and the collective pitch commands during force disturbance provided by the swashplate itself.

In the appointed research program, [3] presents a fly-by-wire architecture controlling the pitch mechanism of the main rotor based on a quadruplex electrical and dual hydraulic system, while this paper deals with the modeling of the variable pitch mechanism, that is fundamental in order to analyze the fly-by-wire system performance.

Given the pilot commands and flight conditions, feathering angle on the blades and force feedbacks on the swashplate actuators have been calculated, through the study of kinematics and dynamic equilibrium of each link of the system. The modeling methodology of a reference helicopter main rotor has been shown in [4], where a rigid main rotor has been analyzed by solving equilibrium equations of each component of the system. The same analysis could be performed through a dedicated multibody modeling software.

This paper applies the same methodology to a more complex and similar to actual mechanisms helicopter rotor, that is a fully articulated one. In other words, the blades are allowed to perform flapping and lagging motions, besides the feathering one. The following paragraphs present a description of the multibody approach applied to this mechanism model, whose flow of data requires the use of a multibody software in order to overcome algebraic loops and simulation failure.

The model should satisfy the following main requirements: multibody approach ([5] [6]) taking into account all the mechanisms bodies, joints and interactions; model able to work out kinematic and dynamic analysis to evaluate the forces on the swashplate actuators during stationary and transient conditions; model suitable for numerical simulations as well as real-time implementation on hardware-in-the-loop test bench for actuator development; open algorithm model for more detailed analysis and in-deep components contents definitions.

In order to demonstrate the validity of the above described multibody approach, the last part of the paper presents a case study. Inertial, geometric and aerodynamic data has been imposed and significant outputs, like force feedbacks on the swashplate actuators and rotor thrust and torque, have been evaluated during typical helicopter hovering manoeuvres. Deeper analysis concerning existing helicopters will be presented in future works.

2 Reference helicopter rotor and swashplate mechanism

A helicopter fully articulated rotor is represented in figure 1. The hinge succession adopted in the present analysis is the flapping – lagging – feathering one. The base 1 represents the fuselage, while the main rotor is composed by the shaft 2, the flapping and lag links 3 and 4, and the blades 5. The pitch orientation of each blade is controlled by the swashplate mechanism through the pitch rod 8. However, some coupling is present among flapping, lagging and feathering motion and the pilot command on the swashplate does not control the pitch angle univocally. The swashplate, composed by the rotating plate 7 and non-rotating plate 6, is connected to the rotor shaft through a spherical pair and a slider. Moreover, an upper drag-arm makes the shaft and the rotating swashplate 7 revolve together, as well as a lower drag-arm connects the non-rotating swashplate 6 to base 1. This arrangement enables the swashplate to slide in a direction parallel to the rotor axis and also to rotate about two axes in its own plane. The position and orientation of the swashplate is completely set by a number of actuators.

3 Kinematics of the mechanism

The study of the kinematics of the system passes through the definition of the position and orientation of each component. The coordinate reference systems of each body are shown in figure 1. First of all, a world coordinate reference frame CS0 is set on the ground. The

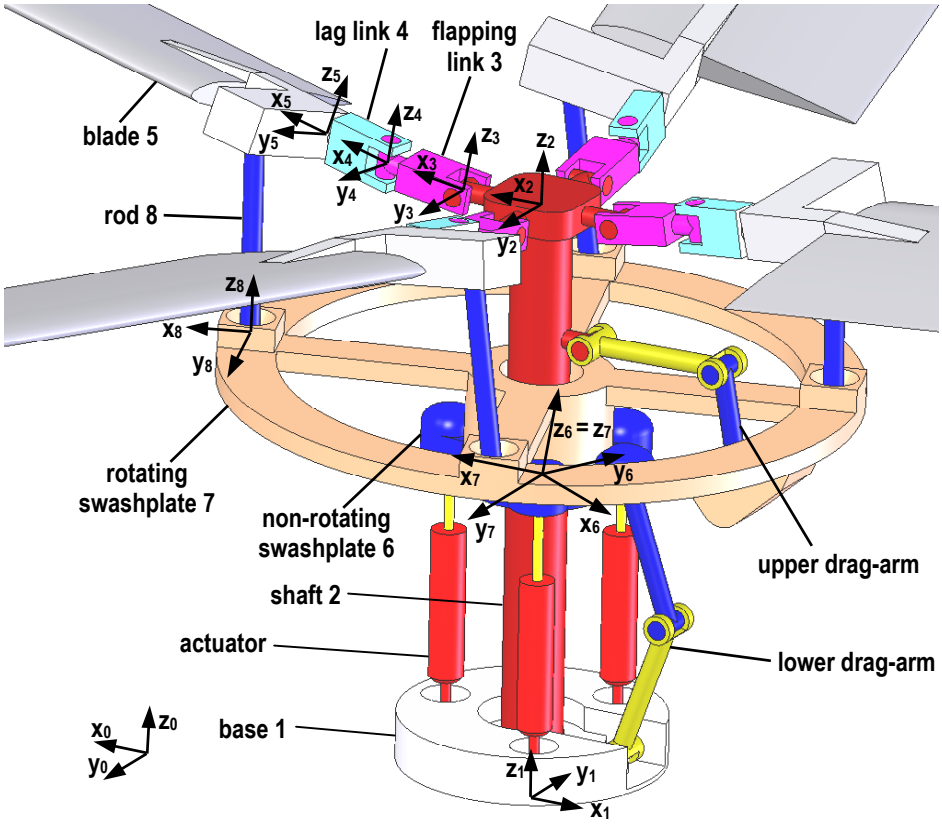

Fig. 1. Rotor helicopter mechanism and coordinate reference frames.

reference system CS1 is fixed to base 1: the x axis is directed towards the tail of the fuselage and the z axis overlaps with the main rotor axis, pointing towards the top of the machine. The reference system CS2, located on the rotor shaft 2, can be obtained from CS1 translating the latter along z_1 axis and rotating it of the azimuth angle ψ, that is the angle of rotation of shaft 2.

The flapping hinge axis coincides with y_3 axis of CS3, that identifies link 3 location and whose orientation is defined by β flapping angle. Similarly, z_4 axis of CS4, that is associated with link 4, identifies the lag hinge axis: its rotation angle is the lag ξ angle. The third main rotor hinge is the feathering one: its axis is defined by x_5 axis belonging to CS5, the reference system associated with the blade. Its orientation is defined with respect to CS4 through pitch angle θ. Moreover, the blade is linked to the swashplate through rod 8, whose position and orientation are represented by CS8. All the previous reference frames have to be repeated for each blade. Link 7 and link 6 are associated with CS7 and CS6, respectively. The former rotates about z_7, that coincides with z_6, of the angle $\psi+\varepsilon$, where ψ is the azimuth angle and ε is a deviation due to the presence of a cyclic tilt of the plate. In fact, CS6, that represents the non-rotating swashplate, can perform a translation along z axis, named as h, and two rotations about y and x axes, referred to as δ and γ, with respect to CS1, in accordance with the kinematic constraints acting on link 6.

4 Multibody explanation

The whole system goal is to determine the forces exerted on the swashplate actuators, according to the pilot pitch commands and flight conditions. Two parallel kinematic architectures are recognizable in the system: the first involves the non-rotating plate, that is connected to the fuselage through the actuators, while the second is made up by each closed kinematic chain that, given the shaft and the rotating plate position, locates the blade through the flapping and lag links and through pitch rod 8.

A block diagram of the multibody model is shown in figure 2. The links are identified by their geometry and inertial parameters, while the

blades are modeled by means of inertial characteristics and aerodynamic data. Additionally, damping or friction effects on the hinges connecting contiguous links can be taken into account.

Kinematics and dynamic equilibrium are solved for each link: frame location, velocity and acceleration are evaluated and they are collected in the proper K signal. Forces and torques data are also determined: they are contained in an appropriate W signal, that is a wrench exerted between subsequent links.

The lower architecture considers as inputs the cyclic and collective pitch commands imposed by the pilot: given this degree-of-freedom (DOF) sequence, the inverse kinematics block provides the reference signal x_{REF} relative to the actuators lengths. The information on the actuators desired lengths goes to the servoactuators block, which gives the actuators actual position, contained in K_A signal. The next step is the calculation of the lower plate direct kinematics: the determination of K_6, together with the shaft velocity information, permits to solve the upper plate kinematics K_7. It is important to note that the upper drag–arm has just been considered as a kinematic constraint on link 7, i.e. it does not transmit any force.

On the other side, shaft velocity and fuselage motion inputs permit to solve the kinematics of the shaft K_2 and, through the flapping and lag links, to determine K_3 and K_4. The latter, together with K_8, that comes from K_7 through the pitch rod, imposes the instantaneous feathering angle of each blade. The aerodynamic loads W_{AER} applied to the blades, that are function of their kinematics K_5, are evaluated and the solution of the dynamic equilibrium of the blades provides the force feedbacks W_{54}, W_{43} and W_{32} through the links and hinges of the chains which connect the blades to the rotor shaft. On the other hand, the force feedbacks W_{58}, W_{87} and W_{76} through the pitch rods and the swashplate permit to determine the force disturbance W_A to the servoactuators.

Moreover, the kinematic and dynamic model of the rotor, combined with a dynamic model of the fuselage, is able to work out the actions applied by the rotor to the fuselage: rotor thrust and torque reaction on the rotor

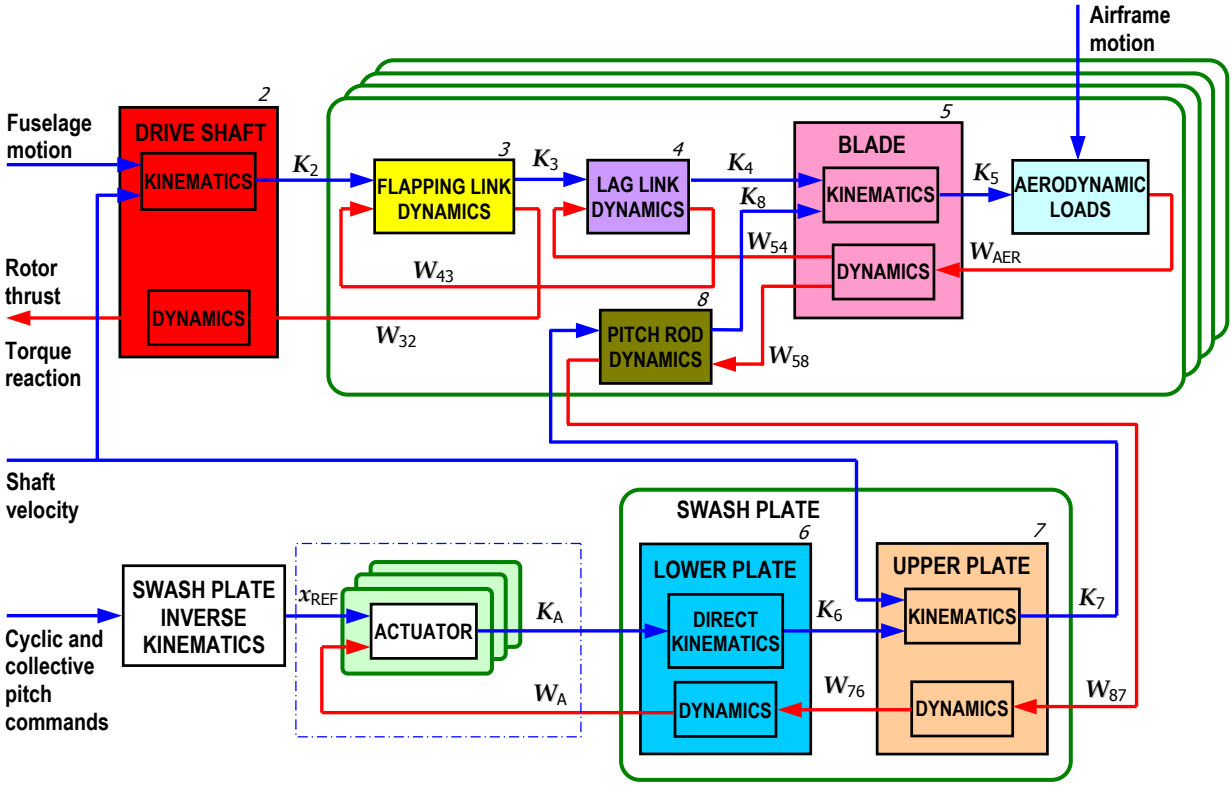

Fig. 2. Block diagram of the multibody model

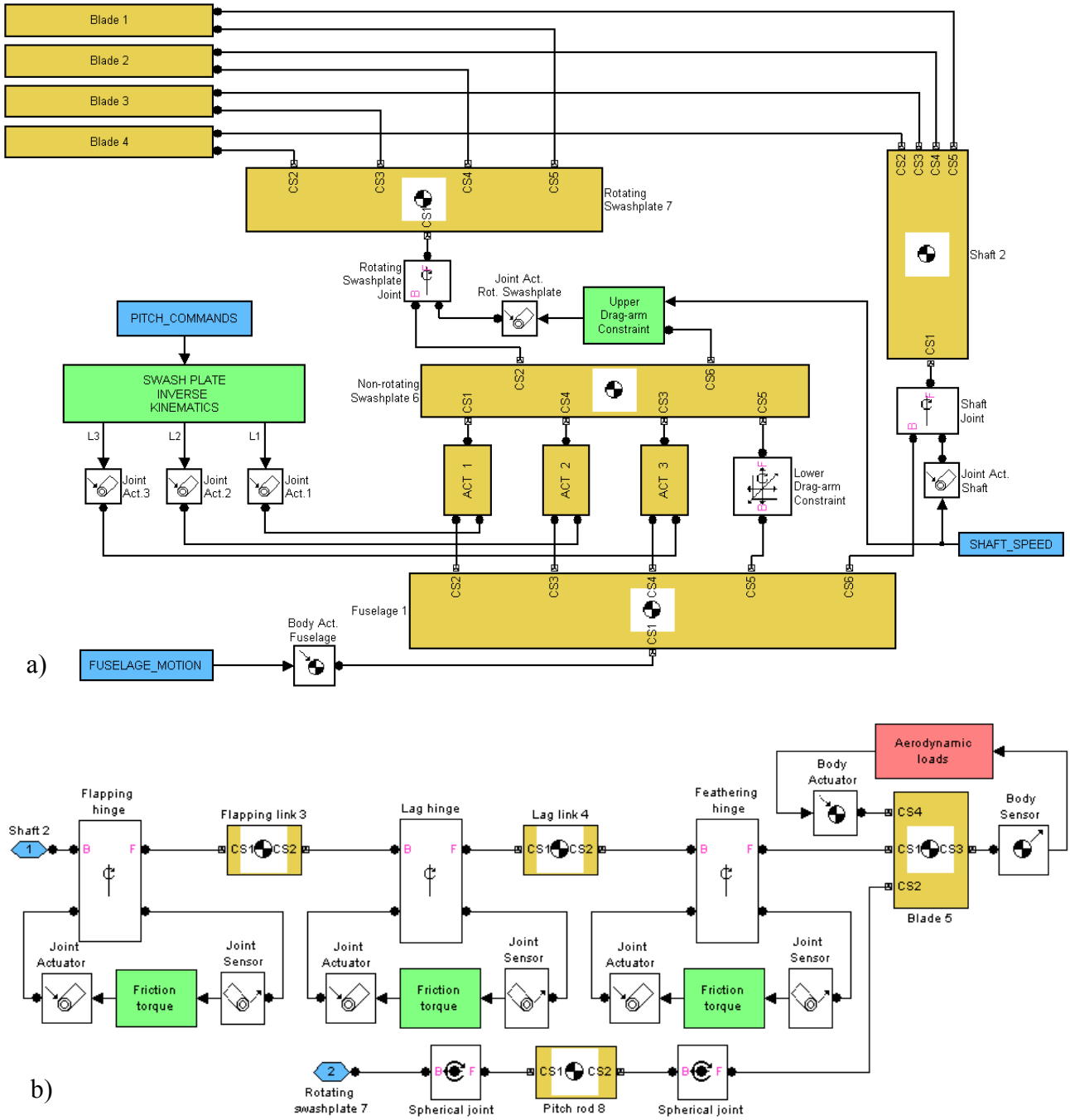

Fig. 3. SimMechanics multibody entire model (a) and blade block detail (b).

shaft can be obtained as functions of the pilot commands and flight conditions, as well as motion of the rotor links and total forces and torques in the mechanism.

5 Calculation details

The logical scheme shown in figure 2 has been implemented on Matlab - SimMechanics multibody software: figure 3a provides the model representation. The fuselage motion input provides the kinematics of the fuselage itself: the swashplate actuators are connected to this link and they receive a reference length signal from the inverse kinematics block through specific joint actuators. In fact, the collective and cyclic pitch commands imposed by the pilot, named as h, δ and γ, are transformed into the corresponding reference length $\boldsymbol{L_i}$ of the i^{th} actuator by the mechanism inverse kinematics

block.

In the following scalar terms are in italics, while vectors are in bold fonts. The generic vector ${}^{i}\boldsymbol{v}$ is intended to be expressed with respect to the i^{th} coordinate reference system.

The inverse kinematics algorithm gives:

$$\boldsymbol{L}_i = -\boldsymbol{a}_i + h\boldsymbol{k}_1 + {}^{1}R_6\,{}^{6}\boldsymbol{b}_i \qquad (1)$$

where $\boldsymbol{a}_i$ is the position vector from CS1 origin to the joint between the fuselage and the i^{th} actuator; $\boldsymbol{b}_i$ is the position vector from CS6 origin to the joint between the same actuator and plate 6; ${}^{1}R_6$ is the orientation matrix of CS6 with respect to CS1, that is function of δ and γ; $\boldsymbol{k}_1$ is the unit vector along z_1. The vectors are intended to be expressed in CS1 unless otherwise specified.

As seen in the previous paragraph, the knowledge of the actuators actual length, that results from the reference one, together with the presence of a constraint that represents the lower drag-arm and the spherical joint and slider, permits to solve the kinematics of the non-rotating plate. Link 7 rotates with respect to link 6, thanks to the presence of the upper drag–arm, that has been considered just as a kinematic constraint on rotating plate, i.e. it does not transmit any force. As previously stated, the orientation of CS7 with respect to CS6 can be expressed through the angular DOF $\psi+\varepsilon$, where the deviation ε is a function of the cyclic command and the azimuth angle; it is:

$$F_1(\delta,\gamma,\psi)\,cos(\varepsilon) + F_2(\delta,\gamma,\psi)\,sin(\varepsilon) = 0 \qquad (2)$$

where F_1 and F_2 are functions of the mentioned parameters [4].

On the other hand, the fuselage is connected to the shaft through a revolute joint, actuated by the shaft velocity input. Each blade block is connected to the shaft and to the rotating plate. Figure 3b shows this subsystem: the feathering hinge connects the blade to link 4, that is connected to link 3 through the lag hinge. Finally, the flapping hinge connects link 3 to the rotor shaft. Friction and damping actions have been assumed in the modeling of the rotor hinges. The damping action is particularly significant on the lag hinge, due to the presence of a physical damper on existing helicopter rotors; in the model, the effects of the damper are modeled with a viscous torque simply proportional to the relative angular velocity between the flapping and the lag links. Moreover, the blade is connected to the swashplate through a pitch rod: spherical joints have been inserted in order to connect these bodies.

At this point, the knowledge of blades kinematics allows to determine the aerodynamic loads acting on the main rotor ([7], [8]). A first approach for estimating aerodynamic actions consists in applying the results given by the actuator disc theory (ADT). It describes the performance of the rotor by means of simple momentum methods. In fact, the thrust T exerted by the rotor can be explained as the variation of the momentum of the mass of moving air that is part of the rotor slipstream. According to ADT, if the velocity of the moving air through the actuator disc in hovering state is the induced velocity u and the air mass flow through the same disc is $\dot{m}$, then it is:

$$T = 2u\dot{m} \qquad (3)$$

If ρ is the air density and R is the blade length, it becomes:

$$T = 2\rho\pi R^2 u^2 \qquad (4)$$

Another approach, named as the blade element theory (BET), considers the lift characteristics of the blade regarded as an aerofoil. If C_L and C_D are the lift and drag coefficients of the blade whose chord is c, then the aerodynamic action $\boldsymbol{dF_a}$ on the infinitesimal section of width dr can be decomposed into a parallel to total velocity $\boldsymbol{V_{TOT}}$ lift contribute $\boldsymbol{dL}$ and a perpendicular to $\boldsymbol{V_{TOT}}$ drag action $\boldsymbol{dD}$; it is:

$$\begin{aligned} dL &= \frac{1}{2}\rho V_{TOT}^2 C_L c\,dr \\ dD &= \frac{1}{2}\rho V_{TOT}^2 C_D c\,dr \end{aligned} \qquad (5)$$

According to the notation of figure 4, θ_i is the pitch angle of the generic blade section, that is the rotation about x-axis between lag link CS4 and the local $CS5_i$, that comes from the global blade CS5 through the local twist angle.

The incidence angle α expresses the angle between vector $\boldsymbol{V_{TOT}}$ and axis y_{5i}. Hence, the aerodynamic action can be equally decomposed into a term $\boldsymbol{dF_t}$, parallel to plane x_4y_4 of the lag link reference frame, and a perpendicular to the same plane $\boldsymbol{dT}$ term; it is:

$$\begin{aligned} dT &= dL\ cos(\vartheta_i - \alpha) - dD\ sin(\vartheta_i - \alpha) \\ dF_t &= dL\ sin(\vartheta_i - \alpha) + dD\ cos(\vartheta_i - \alpha) \end{aligned} \qquad (6)$$

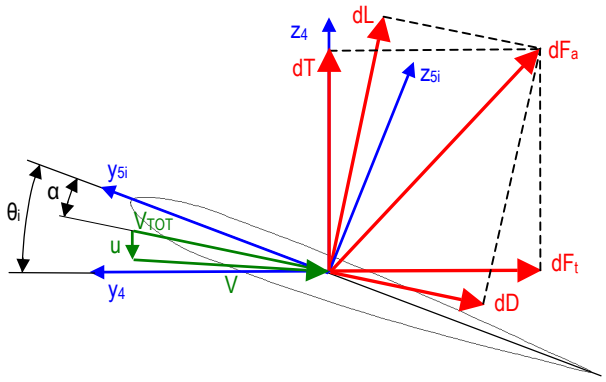

Fig. 4. Force components on blade section.

Since the aerodynamic forces acting on the blade are function of $\boldsymbol{V_{TOT}}$, that is hugely variable along the blade length, it is necessary to arrange a proper discretization of the blade along its radial length. Each element, that will be Δr wide, will be characterized by a unique $\boldsymbol{V_{TOT}}$ and a consequent aerodynamic force will be applied in the element aerodynamic center.

The calculation algorithm imposes that the thrust exerted by each single blade discrete element according to BET gives the same result that can be obtained on the same element according to ADT. In other words, the induced velocity value that gives the convergence between ADT and BET has to be found: this method permits to get the correct thrust for each blade discrete element, under the hypothesis of thrust $\boldsymbol{\Delta T}$ and induced velocity $\boldsymbol{u}$ perpendicular to plane x_4y_4. Figure 5 expresses the logic at the base of this algorithm: on one hand, the induced velocity guess value permits to determine the discrete element thrust according to ADT; on the other hand, the same information, summed to the blade element velocity $\boldsymbol{V}$, gives the total air-to-blade velocity $\boldsymbol{V_{TOT}}$, known in module and direction. The next step is the determination of C_L and C_D coefficients, known as functions of incidence angle α and the Mach number. At this point, lift and drag forces can be calculated and the thrust value according to BET can be obtained through angle θ_i, that represents the information of the orientation of the blade discrete element. Given a threshold limit ε, if $|\Delta T_{BET} - \Delta T_{ADT}| < \varepsilon$, hence the convergence between BET and ADT has been obtained and the actual value of the parameter u is the correct value; otherwise the procedure needs to be repeated with a different value of the induced velocity. A bisection algorithm has been implemented in order to reach the convergence within a few steps.

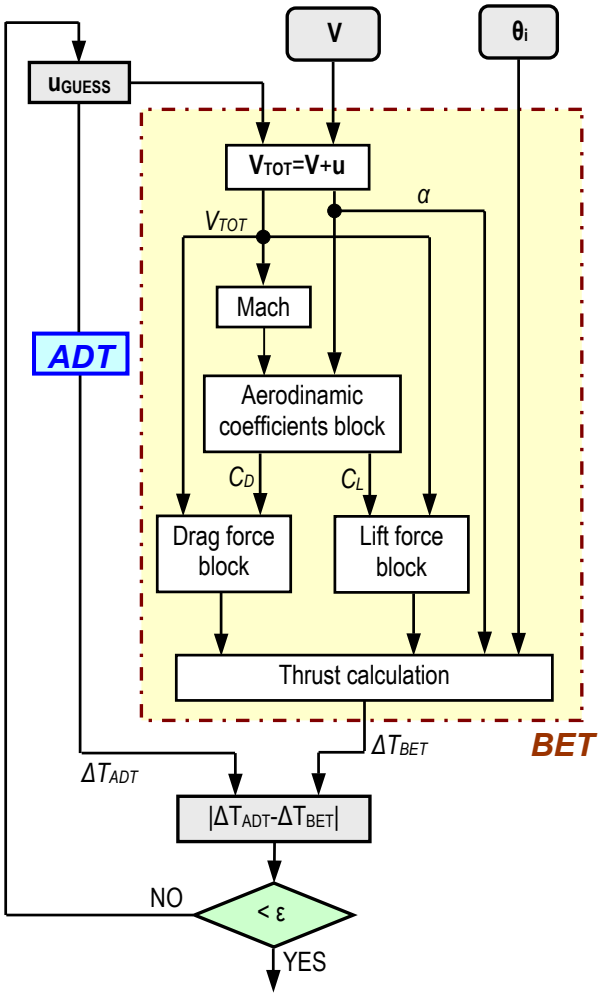

Fig. 5. Aerodinamic actions calculation algorithm

Finally, the determination of the aerodynamic loads, together with inertial and geometrical data, permits to solve the dynamic equilibrium of all the links involved in the

multibody model: force actions on the actuators, as well as rotor thrust and torque reaction, can be evaluated as functions of the pilot commands and flight conditions.

6 Simulation results

The kinematic and dynamic model has been tested using data of a representative helicopter model. In fact, geometry, inertial properties and aerodynamic data are referred to the Sikorsky Uh-60A Black Hawk [9] [10]. However, a lot of data was not available and only an estimate of it was possible to do: hence, outputs of the model have to be considered significant in their trend while their numeric values do not refer to any specific helicopter type. In other words, the following graphs are to be intended as a proof of the validity of the mathematical and logical method that is implied in the previously exposed multibody model. Exhaustive analysis of the helicopter main rotor model outputs will be presented in future works, when thorough data concerning existing rotary wing aircrafts will be available.

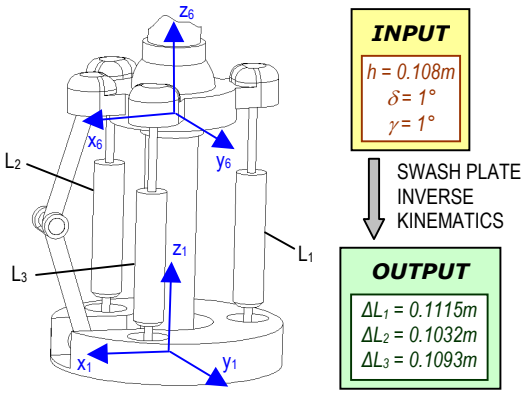

Fig. 6. Swashplate configuration adopted for the simulations.

As previously stated, the inputs of the model are the flight conditions, the rotor shaft velocity and the collective and cyclic pitch commands. In the following simulations the helicopter has been supposed to be in hovering condition, while the rotor shaft velocity $\dot{\psi}$ has been set equal to 27 rad/s, as derived from the reference helicopter. The collective and cyclic pitch commands are both different from zero: the h translational DOF concerning the non-rotating plate has been set to 0.108 m from the reference position, while the δ and γ angular DOFs have been posed equal to 1°. Figure 6 shows the non-rotating plate configuration: the control system has been supposed to be composed by three prismatic actuators, placed at 120 degrees each other. Actuators are labeled as L_1, L_2 and L_3, according to the figure notation. Cyclic and collective pitch pilot commands, that are link 6 DOFs, determine the actuator length variation through the swashplate inverse kinematics algorithm, as previously stated. It is noticeable that the outcomes of the simulations resulting from these numeric values are a direct consequence of the adopted geometric dimensions and they do not have a general validity.

A first output that can be studied is the kinematics of a blade: the results are shown in figure 7. The imposition of a combined cyclic and collective pitch command correctly gives a feathering angle that presents a sinusoidal trend with a mean value different from zero. This $\theta_{0.75}$ angle is the orientation angle of the blade section that is placed at 75% of the blade length: it derives from the θ angular DOF, which defines CS5 orientation, combined with the blade twist at that radial location. A similar trend is also presented by the flapping and lag motion, even if there is a phase displacement among them. It can be noted that the maximum feathering angle roughly corresponds to the maximum flapping angular velocity, i.e. the plane defined by the swashplate has about a 90° phase lead with respect to the tip path plane. For

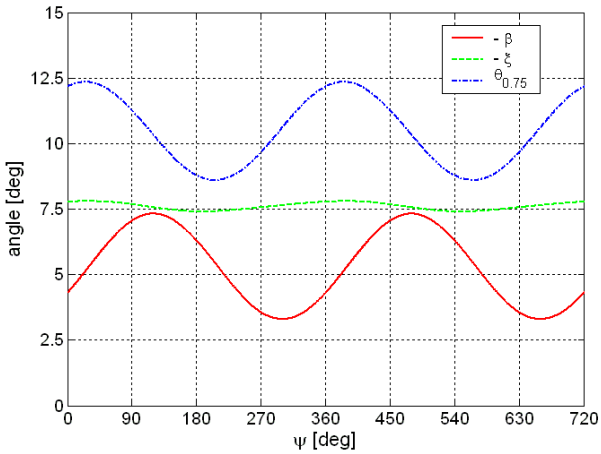

Fig. 7. Kinematic DOFs of the first blade of the rotor as functions of the azimuth angle.

sake of compactness, the flapping and lag angles reproduced in the figure are the opposite of β and ξ angles, whose actual values are negative.

Other noteworthy outputs pertain to the dynamic aspects of the model: the rotor thrust and torque reaction are shown in figures 8 and 9, where the local pitch angle $\theta_{0.75}$ of the first blade of the main rotor is also reproduced (the first blade is the one that points in the x-axis direction relative to CS2). Both the rotor thrust and torque reaction have an about sinusoidal trend with a circular frequency that is twice the circular frequency of the pitch rate variation. However, the amplitude of the oscillations is quite small.

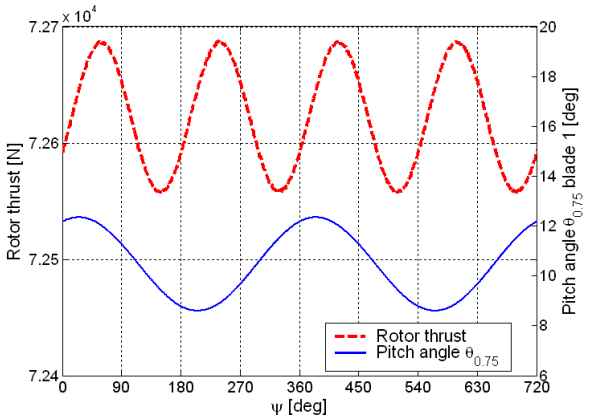

Fig. 8. Main rotor thrust as function of the azimuth angle.

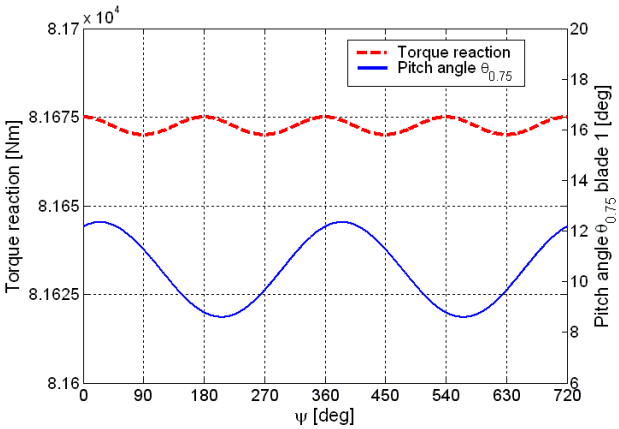

Fig. 9. Torque reaction on the rotor shaft as function of the azimuth angle.

Finally, figure 10 shows the trend of the force actions transmitted to the servoactuators L_1, L_2 and L_3. The pitch angle $\theta_{0.75}$ of the first blade of the main rotor is also reproduced. Firstly, it can be noted that these actions have the same sinusoidal trend, as described above. Secondly, the actions that are required to the actuators are quite different each other, because of the asymmetry introduced by the cyclic command: more elongated is an actuator with respect to the others, bigger is the required action.

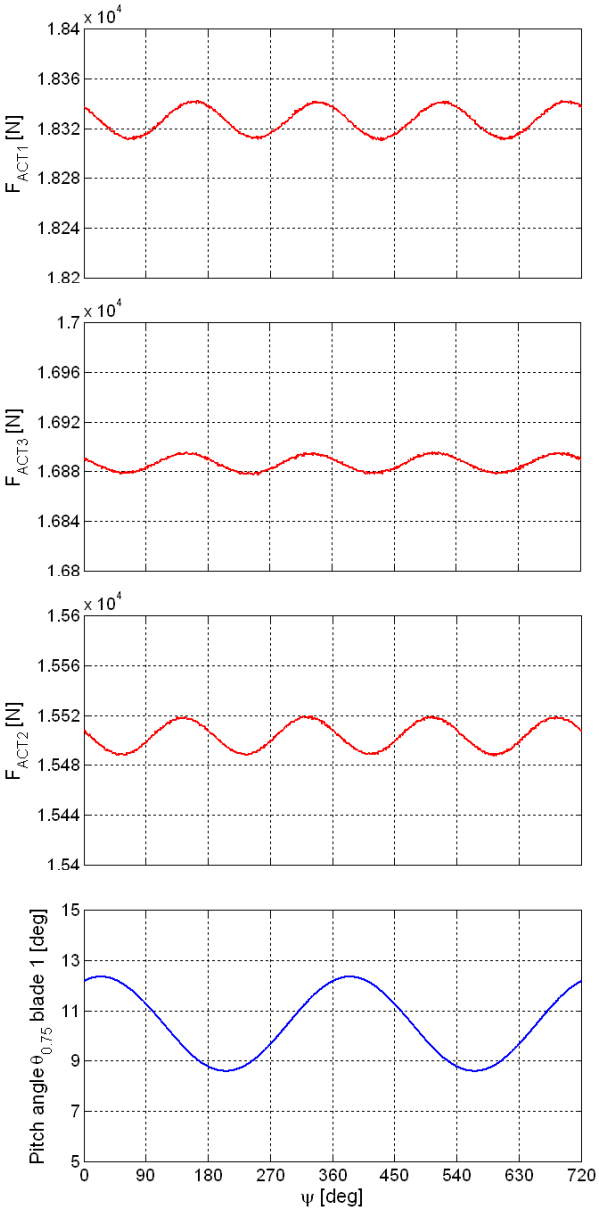

Fig. 10. Actions required to the actuators as functions of the azimuth angle.

7 Concluding remarks

A multibody model aimed at analyzing kinematics and dynamics of a helicopter main rotor has been presented in the paper. It allows

numerical simulation of the behavior of a fully-articulated rotor assuming as inputs the collective and cyclic pitch commands, rotor shaft velocity and motion of the fuselage. Given these inputs, blades kinematics is solved through the knowledge of the swashplate and flapping and lag links motions. Then aerodynamic loads and inertial characteristics of the blades are evaluated and the solution of the dynamic equilibrium of the blades allows to work out force feedbacks through the links and hinges connecting the blades to the rotor shaft. On the other side, given the force feedback from the blades through the pitch rods, the swashplate dynamic equilibrium analysis leads to forces on the servoactuators which drive the swashplate position and orientation.

Hence, the model of the rotor, combined with a dynamic model of the rotary wing aircraft, is able to work out the actions applied by the rotor to the fuselage, for example rotor thrust and torque reaction, as well as motion of the rotor links and total forces and torques in the rotor mechanism.

The study presented is part of a research program on fly-by-wire architectures for actuation of the main rotor of helicopters: the model developed is an important aid in evaluating force disturbance on servoactuators in order to analyze their performances, both in normal and degraded conditions, that is the transient following a failure. Besides the model is suitable for numerical simulations as well as real-time implementation on hardware-in-the-loop test benches for actuators development.

References

[1] Vidal P.A., NH 90 Helicopter Fly-by-Wire Flight Control System, *Proceedings of the American Helicopter Society 53rd Annual Forum*, Phoenix, pp. 915-923, 1997.

[2] Bassett J., Boczar B., Brinkmeier N., H92 Fly-by-Wire System Integration Laboratory (FBW SIL), *Proceedings of the American Helicopter Society 62nd Annual Forum*, Virginia Beach, Virginia, pp. 467-478, 2006.

[3] Jacazio G., Serena Guinzio P., Sorli M., A Dual-Duplex Electrohydraulic System for the Fly-by-Wire Control of a Helicopter Main Rotor, *Proceedings of the 26th International Congress of the Aeronautical Sciences*, Anchorage, 2008 (in press).

[4] Battezzato A., Pastorelli S., Sorli M., Kinematic and Dynamic Modeling of a Helicopter Rigid Main Rotor, *Proceedings of the ASME 2008 International Design Engineering Technical Conferences & Computers and Information in Engineering Conference*, New York, 2008 (in press).

[5] Lange C., Ranjbaran F., Angeles J., Goritschnig G., The Kinematics of the Swashplate Mechanism of a VTOL Unmanned Aerial Vehicle, *Multibody System Dynamics*, Vol. 3, pp 333-365, 1999.

[6] Lange C., Angeles J., Ranjbaran F., Goritschnig G., The Dynamics of the Swashplate Mechanism of a VTOL Unmanned Aerial Vehicle, *Multibody System Dynamics*, Vol. 5, pp 105-131, 2001.

[7] Prouty R.W., *Helicopter performance, stability and control.* Robert E. Krieger Publishing Co, 1990.

[8] Balmford D., Done G., *Bramwell's Helicopter Dynamics.* 2nd edition, Butterworth-Heinemann, 2001.

[9] Howlett J. J., UH-60A Black Hawk Engineering Simulation Program: Volume I – Mathematical Model, *NASA Contractor Report 166309*, 1984.

[10] Bousman W. G., Aerodynamic Characteristics of SC1095 and SC1094 R8 Airfoils, *NASA/TP-2003-212265, AFDD/TR-04-003*, 2003.

Acknowledgement

The research activity presented in this paper has been supported by a grant provided by the Regione Piemonte of Italy.

Copyright Statement